

Microfluidic cell counter/sorter utilizing multiple particle tracing technique and optically switching approach

Chen-Chen Lin · Angela Chen · Che-Hsin Lin

Published online: 21 July 2007
© Springer Science + Business Media, LLC 2007

Abstract This paper proposes a novel microfluidic system based on a computer controlled digital image processing (DIP) technique and optical tweezers for automatic cell/microparticle recognition, counting and sorting in a continuous flow environment. In the proposed system, the cells/microparticles are focused electrokinetically into a narrow sample stream and are then driven through the region of interest (ROI), where they are recognized and traced in real time using a proprietary DIP system. Synchronized control signals generated by the DIP system are then used to actuate a focused IR laser beam to displace the target cells from the main sample stream into a neighboring sheath flow, which carries them to a downstream collection channel where they are automatically counted. Experimental trials show that the microchip is capable of continuously sorting and counting microparticles with diameters of 5 and 10 μm . In addition, a sample composed of yeast cells and polystyrene (PS) beads is

successfully sorted and collected with a 100% of yield ratio and 91.9% of recovery ratio. The proposed system provides a simple, low-cost, high-performance solution for cell manipulation in microfluidic devices.

Keywords Microfluidics · Microparticle · Digital image processing · Electrokinetic focus · Optical tweezers

Abbreviations

\bar{V}	particle velocity within the electric-driven flow (pixel/s)
\bar{u}	particle velocity in the x -axis direction within the electric-driven flow (pixel/s)
\bar{v}	particle velocity in the y -axis direction within the electric-driven flow (pixel/s)
P	particle position (pixel)
t	time (s)
Δt	time interval between two consequent image frame (s)
η	viscosity of the buffer liquid ($\text{N}\cdot\text{s}/\text{m}^2$)
v	fluid velocity of the electric-driven flow (m/s)
r	radius of particle

The preliminary results of the current paper had been presented at the 5th IEEE Conference on Sensors (IEEE Sensors 2006), Daegu, Korea, Oct. 22–25, 2006.

C.-C. Lin · C.-H. Lin
Department of Mechanical and Electro-mechanical Engineering,
National Sun Yat-sen University,
Kaohsiung 804 Taiwan, Republic of China

A. Chen
Institute of Biomedical Sciences, National Sun Yat-sen University,
Kaohsiung 804 Taiwan, Republic of China

C.-H. Lin (✉)
Advanced Crystal Opto-electronics Research Center,
National Sun Yat-sen University,
Kaohsiung 804 Taiwan, Republic of China
e-mail: chehsin@mail.nsysu.edu.tw

Nomenclature

BOE	buffered oxide etchant
CCD	charge coupled device
DI	deionized water
DIP	digital image processing
FACS	fluorescence-activated cell sorters
HCL	hydrogen chloride
HMI	human-machine interface
IR	infrared
LIF	laser induced fluorescence
MEMS	micro-electro-mechanical-systems
mM	millimolar

N.A.	numerical aperture
PC	personal computer
ROI	region of interest
V	volt

1 Introduction

Integrated microfluidic devices for medical analysis and biotechnical research purposes are a subject of particular interest in the MEMS (micro-electro-mechanical-systems) research field (Shoji 1999). Compared to conventional large-scale systems, microfabricated devices have a number of advantages for bio-analysis applications, including reduced sample and reagent consumptions, a more rapid detection performance, and a greater efficiency. However, in developing microchips for such applications, it is generally necessary to combine several functions (e.g. injection, mixing, reaction, and so forth.) on a single chip, and hence the corresponding design and fabrication tasks are both complicated and expensive. Consequently, a requirement exists to develop low-cost, straightforward microfluidic systems capable of the automatic handling of microparticles and other bio-particles in continuous flow environments. In biomedical analysis applications, it is commonly necessary to extract the cells of interest from a large mixed population such that they can be processed in some way. Accordingly, microfluidic devices for such applications are generally designed to carry out three basic procedures, namely target particle detection, sorting and counting. Many miniaturized cell/particle sorters have been presented in the literature (Fiedler et al. 1998; Li and Harrison 1997). However, these devices typically comprise delicate moving parts and/or actuators and require complex fabrication procedures. As a result, they are incompatible with the general trend toward low-cost, disposable products.

Cell manipulation and separation is an essential requirement in many bio-analytical applications (Holmes et al. 2006; Yi et al. 2006). These tasks are conventionally performed using large-scale flow cytometers (Edwards et al. 2004). However, such systems are bulky, expensive and not easily accessed. Accordingly, various optical methods have been proposed for miniaturized cell/particle detection systems. Typically, these microscale devices are based upon integrated waveguides and/or optical fibers (Holmes et al. 2006; Lin and Lee 2003; Lin et al. 2004; Mio et al. 2000). Although the resulting optical devices are capable of detecting micro-sized particles with a very high degree of accuracy, and can achieve a high throughput, the corresponding fabrication procedures are highly complex and time-consuming. Ashkin et al. 1986 demonstrated the trapping of dielectric particles using a single-beam gradient

force. Since then, optical tweezing has emerged as a powerful technique for manipulating microparticles at the cell scale. Enger et al. 2004 applied an optical manipulation technique to carry out cell sorting in a microchannel. In the proposed approach, the target cells were captured using a focused laser beam and were then ejected from the main sample stream into a neighboring sheath flow. However, the device throughput was limited since manipulation was performed on a cell-by-cell basis. To address this limitation, Wang et al. 2005 presented a microfluidic device for the continuous sorting of mammalian cells based on an optical force switching technique. The results showed that the device was capable of achieving a throughput of 20–100 cells/s (Wang et al. 2005). However, the device was based on a laser induced fluorescence (LIF) detection scheme, and was therefore applicable only to the sorting of fluorescence-labeled objects.

Digital image processing (DIP) provides a powerful tool for segregating moving objects from a static background without the need for delicate pretreatment procedures such as those required in LIF methods (Lee et al. 2005; Maerz 1998). Therefore, DIP provides an ideal enabling technology for the controller unit of active optical tweezer systems. Detecting biological cell samples using an image analysis approach involves determining their various diagnostically important parameters and patterns, e.g. their size, shape and texture. Obtaining accurate measurements of cell parameters with the assistance of computer-aided image processing systems has become common practice in quantitative pathology and medical applications (Wu et al. 1998). Nowadays, digital image processing is a rapidly evolving field with a growing number of applications within the basic cell biology and clinical medicine research fields (Vajda 1994). Wietzorrek et al. 1994 presented a flow cytometric imaging technique for the identification of marine organisms, in which a novel method referred to as “Imaging in Flow” was used for the simultaneous imaging of selected objects. Fu et al. 1999 presented a disposable cell sorting device. In the proposed approach, the conventional flow chamber used in fluorescence-activated cell sorters (FACS) was replaced with a microfabricated device which provided the advantages including higher optical detection sensitivity, an easier mechanical setup, and an improved sorting capability.

The current study integrates an electrokinetic focusing method, a proprietary DIP system and IR laser tweezers to develop a microfluidic system for automatic cell sorting and counting applications in a continuous flow environment. In the proposed approach, the cell samples are detected, recognized and traced in the microchannel using the DIP system. Based on control signals generated by the DIP system, the traced target cells are then switched automatically into a neighboring sheath flow by the optical laser tweezers. Finally,

the target cells are carried to a downstream collection channel, where they are automatically counted. The flow field in the microfluidic device is visualized using both numerical and experimental methods. The effective trapping force of the optical tweezers is evaluated using a simple form of the Stoke's drag equation. Experiments are performed to investigate the effect of the laser output power on the maximum flow velocity, the effective trapping force, and the particle displacement, respectively, for particles of different sizes. Finally, an automatic cell sorting and counting process is demonstrated.

2 Working principle

Figure 1 presents a schematic illustration showing the basic working principles of the proposed automatic cell sorting and counting system. Particles are introduced into the microfluidic system and are focused electrokinetically into a narrow sample stream which then flows through the region of interest (ROI). A high speed CCD camera is used to capture images of the particles as they pass through the ROI and a proprietary DIP method is then used to carry out multiple particle detection, recognition and path tracing. Signals generated by the DIP system are used to actuate a single beam optical tweezer to extract the target particles from the main sample flow stream and to redirect them to a downstream collection channel, where they are automatically counted. The proposed approach makes possible the continuous sorting and counting of cell samples without the need for any moving parts or embedded transducers. In order to enhance the particle sorting performance, the proposed microfluidic device features an expansion-channel design to increase the separation distance between the different flow streams in the downstream region of the microchannel. Using this simple approach, the lateral displacement of the optically switched cells/particles can be increased significantly.

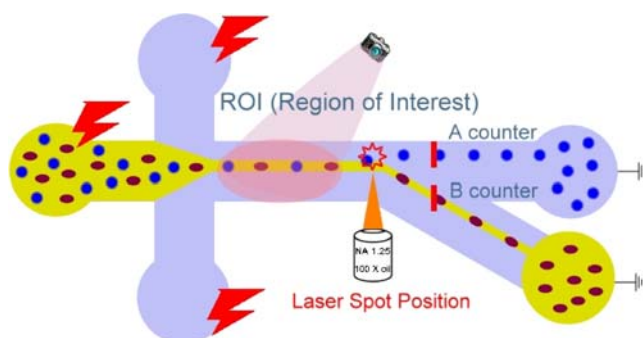


Fig. 1 Design concept of the proposed automatic system for cell sorting

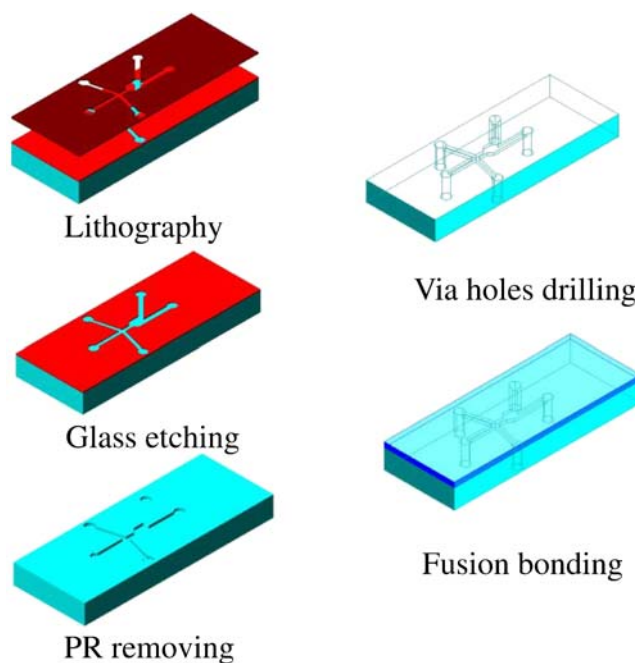


Fig. 2 Schematic representation of simplified fabrication process for microchips

3 Chip fabrication and experimental setup

3.1 Microchip fabrication

Figure 2 provides an overview of the fabrication process used to create the current microfluidic chip. The microchip was fabricated on a low-cost commercially-available microscope glass slide ($25 \times 75 \times 1.0$ mm; Marienfeld, Germany) using a modified glass fabrication process (Lin et al. 2001). To match the effective working distance of the high N.A. objective lens used in the optical tweezer setup, the microchannels in the lower substrate were sealed using a glass cover plate with a thickness of $170 \mu\text{m}$. Prior to the microfabrication process, the two slides were annealed at a temperature of 400°C for 4 h to release residual internal stresses and were then cleaned in a boiling Piranha solution for 10 min. (Caution: Piranha solution is highly corrosive and should be handled with extreme care.) One substrate was then coated first with a thin layer of hexamethyldisilazane (HMDS, J. T. Baker, USA) as an adhesive primer and then with a $3\text{-}\mu\text{m}$ thick layer of AZ 4620 positive photoresist (PR). The substrate was then soft baked, UV patterned and finally immersed in a BOE (6:1) etchant solution. During the etching process, the substrate was removed from the BOE solution every 5 min and dipped in a 1 M HCl solution for 10 s to turn the insoluble precipitate of CaF_2 and MgF_2 into soluble CaCl_2 and MgCl_2 . The etching process was continued for a total of 40 min, resulting in a final microchannel depth of $36 \mu\text{m}$. Meanwhile, the second glass slide was drilled with fluid via-holes. Both plates were then cleaned once again in a boiling Piranha

solution for 10 min. Finally, the two plates were joined using a thermal fusion bonding process performed in a sintering oven at a temperature of 670°C for 5 min with a ramp rate of 5°C/min. Since the upper glass slide was extremely thin and therefore very fragile, the temperature in the sintering oven was maintained at 400°C for 30 min during the thermal ramping process in order to prevent it from cracking during the bonding process.

Figure 3 presents optical images of the completed microfluidic chip. The device has overall dimensions of 2.6×4.0 cm. As shown in the close-up image in Fig. 3(b), the microchannel width expands from 160 to 300 μm at a point 400 μm downstream from the microchannel cross-form intersection. Figure 4 presents the simulation and experimental results for the flow fields in a conventional straight microchannel and in the current expansion channel, respectively. The two sets of results are in good agreement in both cases, and demonstrate that the width of the flow field increases significantly in the expansion region of the current microchannel.

3.2 Experimental setup

Figure 5 illustrates the experimental setup established for the proposed automatic cell sorting/counting system. The sample manipulations in the microchip were observed using a stereo microscope equipped with a high-speed IEEE 1394 interfaced digital CCD camera (75 frame/s, A311fc, Basler, Germany). The captured images were analyzed using a proprietary DIP system. A single programmable high-voltage power supply was used to provide the electrokinetic force required to focus the sample particles and to drive them through the microfluidic channel. The light source for the optical tweezer system was provided by a near-IR laser diode module (808 nm, L808P1WJ, Thorlabs, USA). The laser beam was directed through an objective lens (×100, N.A.=1.25, Olympus, Japan) to produce the optical intensity gradient required to generate an optical trapping force. The laser beam was turned ON/OFF using a computer-controlled shutter system (SH05 and SC10, Thorlabs, USA) regulated by control signals provided by the DIP system. The flow

manipulation experiments were performed using a buffer solution of 10 mM borax ($\text{Na}_2\text{B}_4\text{O}_7 \cdot 10\text{H}_2\text{O}$, pH=9.2, Showa, Japan) and polystyrene (PS) beads with diameters of 5, 10 and 12 μm, respectively (Duke Scientific, CA, USA). During the experiments, the sample stream was focused electrokinetically to a width of 15–20 μm to ensure that the microparticles flowed sequentially through the ROI.

4 Digital image processing protocols

The DIP system used in the current study was based on a proprietary graphical user interface (GUI) constructed using Microsoft Visual Basic. The various sub-programs of the DIP system were integrated using eVision® (EURESYS, Belgium) commercial software. Briefly, the image capture program was coded using Microsoft Visual C++ software using the “Image capture sub-program” modified from Basler’s B-cam Grab Sample Program, while the image display and pattern recognition functions were constructed using Microsoft Visual Basic 6.0 software using the “Image display sub-program” and “Image recognition sub-program” toolkits, respectively. During the experiments, the digital data stream composed of the individual image frames captured using the CCD was acquired using the image capture sub-program. The image data were then transferred to dynamic link library (DLL) files and stored in a shared buffered memory to wait for access requests from the image display and image recognition sub-programs. However, the “multiple particle recognition” and “particle position tracing and velocity measurement” functions developed in the current study are described in the sub-sections below.

4.1 Multiple particle recognition

This study developed two digital image processing techniques, designated as Pattern Match and EasyObject, respectively, to segregate moving objects (i.e. the PS beads) from a static background without the need for delicate pretreatment and fluorescence labeling procedures. Both methods enable the extraction of a single particle from a

Fig. 3 (a) Microfabricated channel device with (b) a close-up view of the microfluidic channel

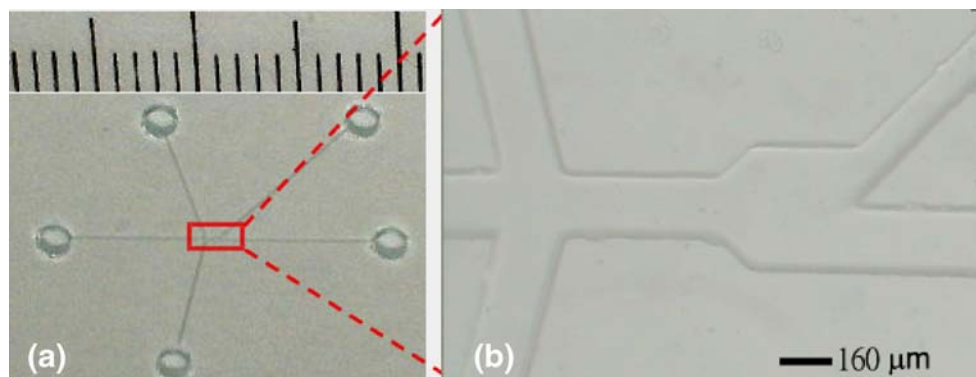
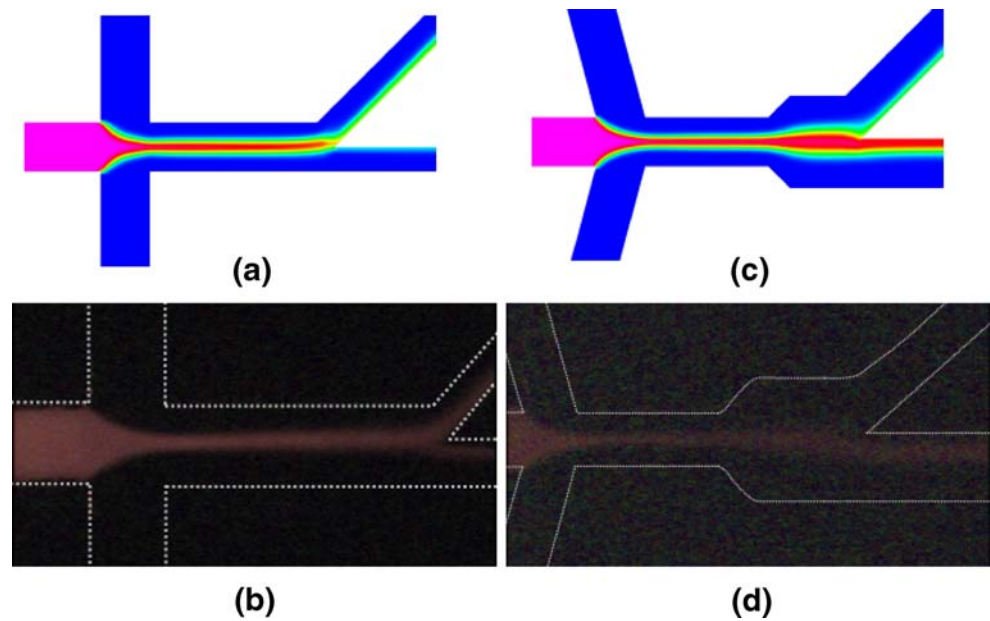


Fig. 4 (a, b) Simulated and experimental results for the flow field of the conventional channel design and (c, d) the new design with expansion chamber

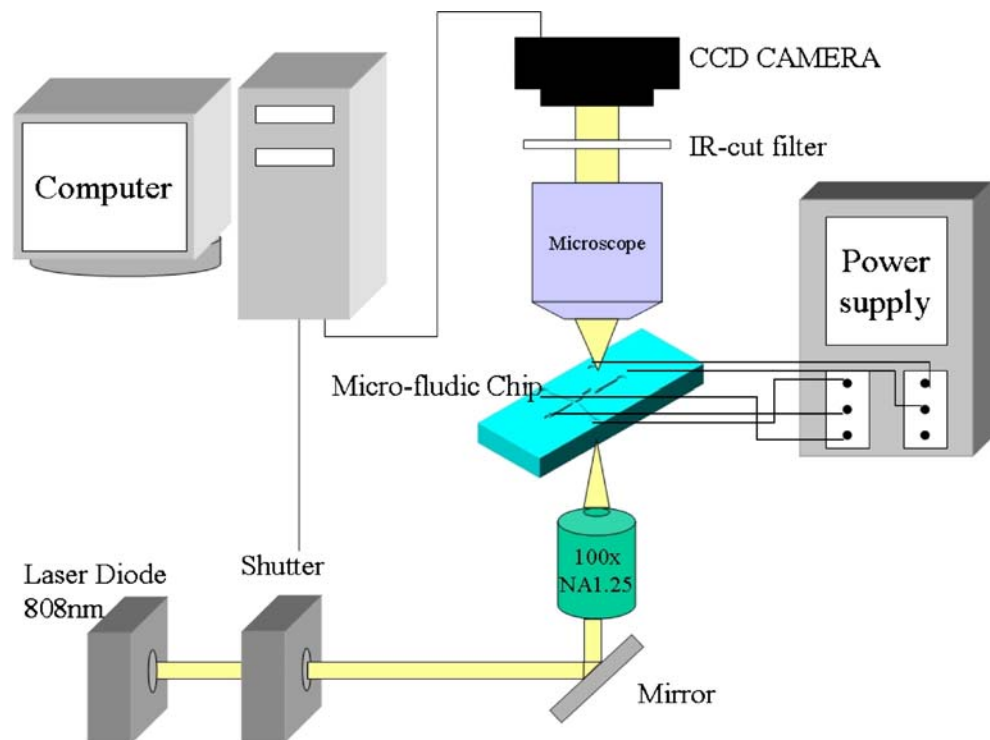


complex but static background. The details of the two methods are described in the following.

1. **Pattern Match.** Figure 6(a) shows the vision recognition results obtained from the Pattern Match routine for the case where the target object is specified as the 10- μm PS particles. Prior to the experiments, the target pattern was “learned” from a specific object. Subsequently, a real-time search was performed for similar patterns in the individual image frames acquired during the experimental procedure. The DIP system then automat-

- ically generated values for the “Score” and “Scale” of each pattern identified by the Pattern Match algorithm, where the score indicated the degree of similarity of the evaluated particle to the learned pattern, while the scale indicated the physical size of the evaluated particle.
2. **Easy Object.** This DIP routine commences by decomposing the image to acquire all of the individual objects present in the frame. In this way, the microparticles can be segregated from the background and processed individually. Each individual object is then expressed in terms of the number of pixels which it occupies in the image. By

Fig. 5 Schematic representation of automatic multiple particle tracing and microfluidic cell counter/sorter system setup



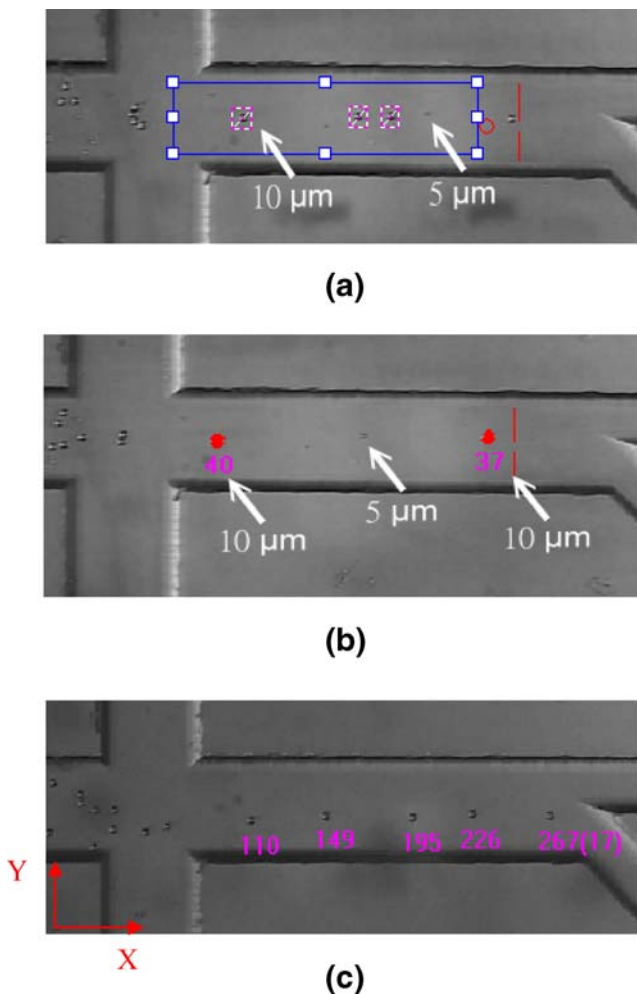


Fig. 6 (a) Multiparticle identification using “Pattern Match” method, (b) successful recognition and tracing of 10- μm particles using “EasyObject” method, and (c) particle position tracing and speed of movement calculation results expressed in units of pixels and pixels/s, respectively

comparing the computed number of pixels with a library containing the pixel area ranges of the different particles of interest, each object identified in the image can be mapped to the corresponding target object. In the current case, the 5- μm particles and the 10- μm particles occupy areas ranging from 10 to 20 pixels and 35 to 45 pixels, respectively. Figure 6(b) presents the DIP results obtained from a multiparticle identification process. The results show that the EasyObject routine successfully recognizes the 10- μm target objects. Note that the data appended to each particle indicate the particle size in terms of the number of pixels it occupies in the image.

4.2 Particle position tracing and moving speed measurement

Once every object in the image has been segregated and identified, their positions and specific features are recorded in each successive “static” image frame. Figure 6(c) presents

typical vision recognition results obtained from a multiple particle tracing and velocity measurement routine. Note that to reduce the image processing time, the DIP system traces the positions of all the recognized objects, but only calculates the velocity of the object closest to the laser-tweezer focus spot. The position and velocity of the objects are calculated at each instant “ t ” using the following formulae:

$$\text{Recognized Objects} \in \{P_t(x, y)_i; i = 1, 2, \dots, n\}, \quad (1)$$

where “ n ” is the total number of cells/particles within the ROI.

The velocity of the object closest to the laser spot is given by

$$\vec{V}_{(t)}(\vec{u}, \vec{v})_i = \left(\frac{d\vec{P}_i}{dt} \right)_x + \left(\frac{d\vec{P}_i}{dt} \right)_y; i = n. \quad (2)$$

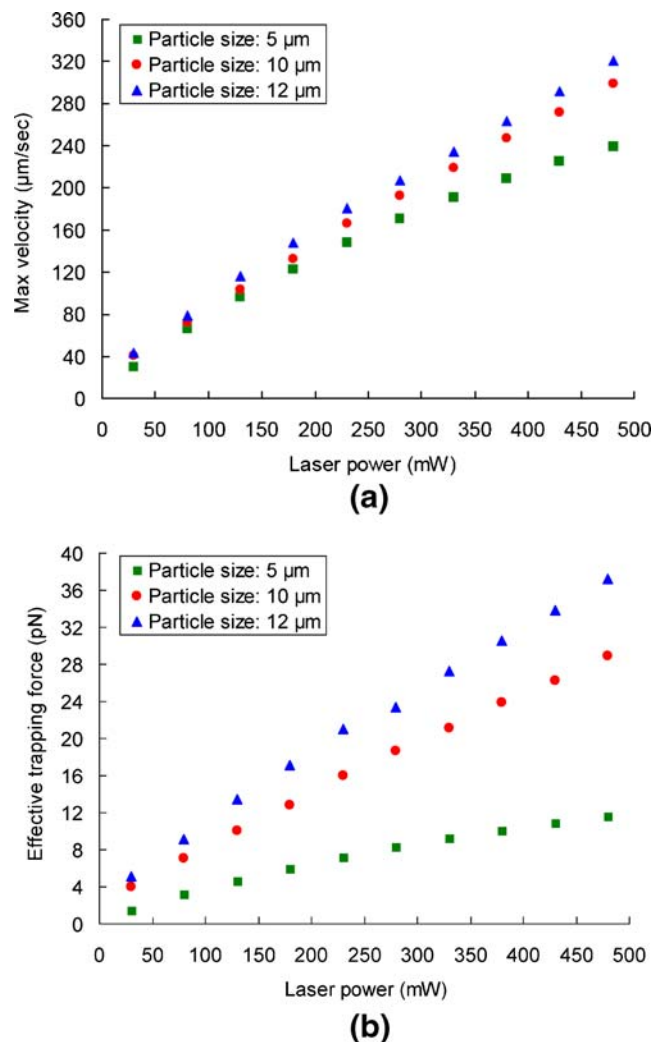


Fig. 7 (a) The relationship between maximum flow velocity and laser trapping power. (b) The relationship between effective trapping force and laser trapping power

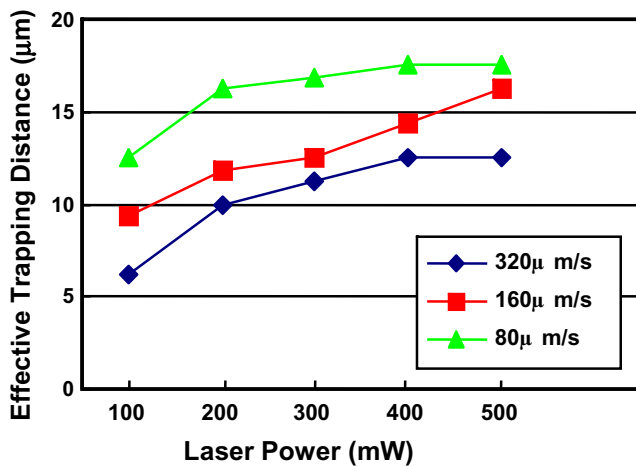


Fig. 8 The relationship between the laser output power and the effective trapping distance on the target particles

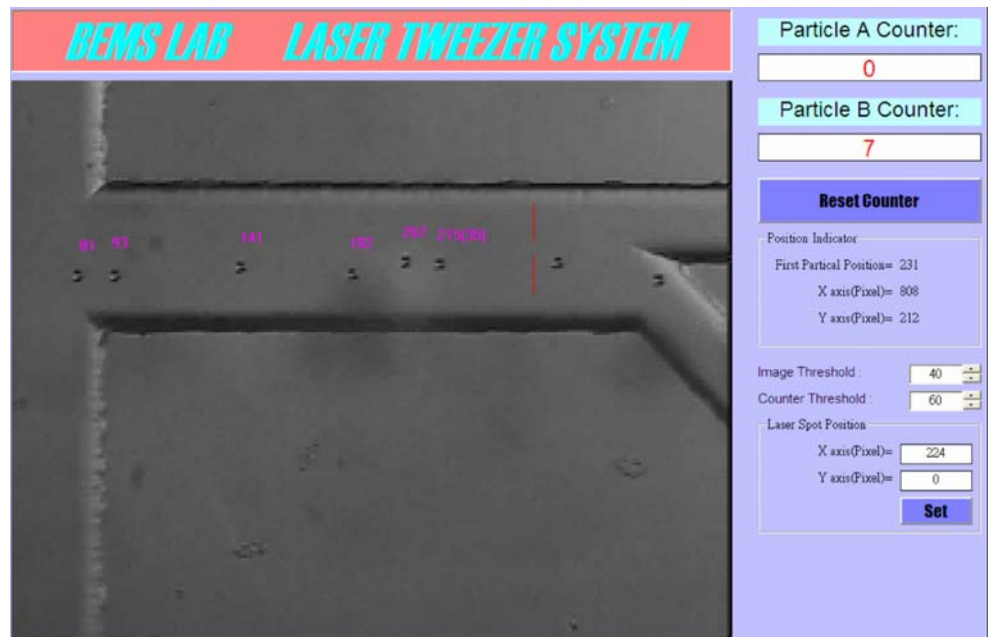
Under the assumption that the cells/particles are well focused and flow sequentially along the center of the flow stream line in the x -direction only, Eq. 2 can be expressed as

$$\vec{V}_{(t+\Delta t)}(\vec{u}, \vec{v})_i = \vec{u}_i = \left(\frac{dP_i}{dt} \right)_x, \tag{3}$$

The interval between two consecutive image frames is given by Δt . Therefore, the velocity (u) of the particle closest to the focus spot can be computed from

$$u_i = \frac{P_{(t+\Delta t)}(x)_i - P_t(x)_i}{(t + \Delta t) - t}. \tag{4}$$

Fig. 9 The HMI (Human–Machine Interface) of proposed real-time automatic sorting and counting system. The value within parenthesis presents the speed of last object in the unit of pixel/s and is attached with the moving objects by vision software program



5 Results and discussion

5.1 Evaluation of the effective force of the laser tweezer

The effective trapping force of the optical tweezer is measured using a modified form of Stoke’s equation. Since the electro-osmotic flow (EOF) in the microchannel is planar and the flow velocity is proportional to the applied electric field strength, a stable Stoke’s drag force acts on the PS microparticles. The relationship between the optical trapping force and the Stoke’s drag force is expressed by

$$F_{\text{cap}} = F_{\text{drg}} = 6\pi r\eta v_{\text{EOF}} = 6\pi r\eta(\mu_{\text{EO}}E), \tag{5}$$

where r is the particle radius, v is the flow velocity, η is the dynamic viscosity of water ($\eta=1.025 \times 10^{-3} \text{ N}\cdot\text{s}/\text{m}^2$), μ_{EO} is the electro-osmotic mobility of the fluid and E is the strength of the applied electric field. To evaluate the effective trapping force, a single PS bead was trapped in the microchannel using the laser tweezer system, and the EOF flow rate was then increased by gradually increasing the strength of the applied electric field. The velocity at which the particle escaped the laser beam (i.e. the so-called maximum flow velocity) was recorded and then substituted into Eq. 5 to compute the corresponding trapping force. Figure 7(a) illustrates the variation of the maximum flow velocity with the laser output power for PS particles of diameters 5, 10 and 12 μm , respectively. Meanwhile, Fig. 7(b) presents the corresponding results for the effective trapping force. In general, the results indicate that the trapping force increases with an increasing particle size. Furthermore, it is observed that the trapping force is of the order of several tens of

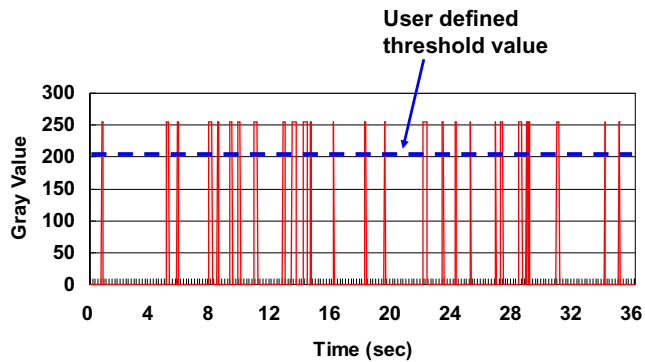


Fig. 10 The counting results of the developed software. Each peak presents a cell/particle that has past the software counter

piconewtons, which is ideal for cell/microparticle manipulation purposes (Fallman et al. 2004; Ishijima et al. 1998).

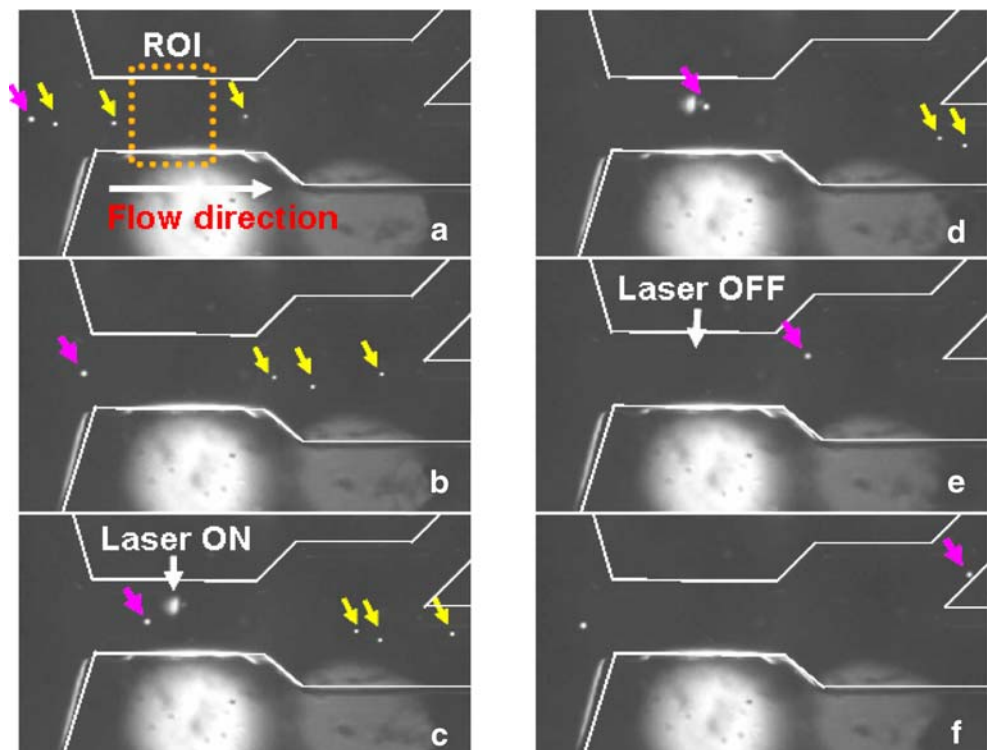
The maximum lateral displacement generated by the optical tweezers was evaluated using PS microparticles of 10- μm diameter. The particles were driven electrokinetically at flow rates of 80, 160 and 320 $\mu\text{m}/\text{s}$, respectively, and their maximum lateral displacement was recorded in each case as a function of the laser power. The IR laser power was set from 100 to 500 mW and the measured effective power was around 70 to 320 mW after the objective lens. Figure 8 illustrates the relationship between the effective trapping distance and the laser output power as a function of the flow rate. The results show that the extent to which the particles are displaced by the laser increases as

the flow rate decreases. Furthermore, for a constant flow rate, the effective trapping distance increases with an increasing laser output power. In general, optical tweezers trap particles at the laser spot, and this obviously causes a problem in continuous cell sorting applications. Therefore, it is important to control the duration of the laser pulse such that it is sufficiently long to divert the target particles from the main sample stream into the neighboring sheath flow, but not so long that the particles become trapped in the laser spot. In the present study, the optimal laser ON duration is calculated to be 250 ms for a particle speed of 320 $\mu\text{m}/\text{s}$.

5.2 Real-time particles tracing, sorting and counting

Figure 9 shows the HMI (human-machine interface) of the proposed real-time automatic sorting and counting system. In this test, EasyObject method was used as the DIP protocol for identifying the target objects. The numbers adjacent to each particle indicate the corresponding x -axis position (in pixels) of the microparticle. As discussed previously, the velocity of the particle closest to the laser spot is also computed in pixels/s. The velocity info is used to synchronize the output pulse of the laser such that the target particles are separated from the main sample stream and directed to the appropriate collection channel. The cells/particles entering the two collection channels are counted automatically using software counter functions embedded in the proprietary DIP system. In the counters, a program loop scans the

Fig. 11 The continuous images of successfully sorting a single 10 μm polystyrene bead out of a mixture of 5 and 10 μm PS samples



gray value changes along the two assigned counting lines in the captured images and a particle is detected (i.e. counted) when the maximum gray value exceeds a predefined threshold value. Figure 10 presents typical counting results for 5- and 10- μm mixing samples.

Figure 11 presents continuous images showing the successful extraction of a single 10- μm PS bead from a mixture of 5- and 10- μm samples. The output laser power was set at 180 mW and the sample flow rate was 300 $\mu\text{m}/\text{s}$ for this test. Initially, the microparticles are aligned along the center of the sample stream by applying an electrokinetic-focusing effect at the cross-form intersection region of the microchip. The particles then flow sequentially through the ROI and are analyzed using the DIP system (Fig. 11(a)). In Fig. 11(a), the DIP system establishes that the particles have a diameter of 5 μm , and are therefore not the target particles. Hence, the laser is not activated, and the particles remain within the sample stream and flow automatically into the lower collection channel (Fig. 11(b)). However, in Fig. 11(c), the DIP system identifies that the particle has a diameter of 10 μm , and hence the laser is actuated to divert this particle from the main sample stream into the neighboring sheath flow. Figures. 11(d)–(f) show that the PS bead is displaced through a distance of approximately 20 μm and then flows into the upper collection channel.

5.3 Yeast sorting test

In order to evaluate the counting performance of the proposed system and method, a mixture composed of yeast cells (3–5 μm in diameter) and the polystyrene beads with 10 μm in diameter was used for counting and sorting test. Pattern match method was adopted for the digital image processing protocol. Yeast cells were the target objects in this test and the sorted yeast cells were collected in the upper reservoir. The operation conditions for laser power and sample flow rate were the same as described above. The total duration of the injection and sorting procedure was 5 min. The sorted yeast cells and PS beads were counted at the upper reservoir and the lower reservoir of the microchip, respectively. The experimental count data for the yeast cells and the PS beads in the upper reservoir and the lower reservoir were 136 yeast cells, 0 PS bead and 12 yeast cells, 272 PS beads, respectively. The calculated yield rate for the yeast cells in the upper reservoir was 100%. However, 12 out of 148 yeast cells were not successfully sorted and collected in this test, resulting in a recovery rate of around 91.9% for the yeast cells. The results indicate that the microchip is capable of sorting target cells with a yield rate of higher than 90%. More importantly, time-consuming process for sample labeling can be excluded using the method proposed in this study such that a high performance sorting of cell/particles can be achieved.

6 Conclusions

This study has integrated an electrokinetic focusing method, a real-time proprietary DIP multiple particle tracing technique and an optical tweezer to accomplish a microfluidic system for automatic cell sorting and counting applications in continuous flow environments. The DIP system automatically identifies the cells/particles of interest as they flow through the ROI, and then actuates the laser tweezers such that these particles are extracted from the main sample flow and directed into a collection channel, where they are automatically counted. Moreover, when applied to the sorting and counting of yeast cells, the proposed system achieves a sorting yield of 100% and a recovery yield of 91.9%. The method presented in this study provides a straightforward and effective solution for cell/microparticle manipulation in the field of micro-total-analysis-systems.

Acknowledgment Financial supports from the National Science Council of Taiwan are acknowledged. (NSC 95-2314-B-110-002-MY3).

References

- A. Ashkin, J.M. Dziedzic, J.E. Bjorkholm, S. Chu, *Opt. Lett.*, **11**, 288 (1986)
- B.S. Edwards, T. Oprea, E.R. Prossnitz, L.A. Sklar, *Curr. Opin. Chem. Biol.* **8**, 392 (2004)
- J. Enger, M. Goksör, K. Ramser, P. Hagberg, D. Hanstorp, *Lab Chip*, **4**, 196 (2004)
- E. Fallman, S. Schedin, J. Jass, M. Andersson, B.E. Uhlin, O. Axner, *Biosens. Bioelectron.* **19**, 1429 (2004)
- S. Fiedler, S.G. Shirley, T. Schnelle, G. Fuhr, *Anal. Chem.* **70**, 1909 (1998)
- A.Y. Fu, C. Spence, A. Scherer, F.H. Arnold, S.R. Quake, *Nat. Biotechnol.* **17**, 1109 (1999)
- D. Holmes, H. Morgan, N.G. Green, *Biosens. Bioelectron.* **21**, 1621 (2006)
- A. Ishijima, H. Kojima, T. Funatsu, M. Tokunaga, H. Higuchi, H. Tanaka, T. Yanagida, *Cell* **92**, 161 (1998)
- G.B. Lee, C.H. Lin, S.C. Chang, *J. Micromechanics Microengineering* **15**, 447 (2005)
- P.C.H. Li, D.J. Harrison, *Anal. Chem.* **69**, 1564 (1997)
- C.H. Lin, G.B. Lee, *J. Micromechanics Microengineering* **13**, 447 (2003)
- C.H. Lin, G.B. Lee, L.M. Fu, B.H. Hwey, *Journal of Microelectromechanical Systems* **13**, 923 (2004)
- C.H. Lin, G.B. Lee, Y.H. Lin, G.L. Chang, *J. Micromechanics Microengineering* **11**, 726 (2001)
- N.H. Maerz, *Proc. 6th Annual Symposium ICAR*, 195 (1998)
- C. Mio, T. Gong, A. Terray, D.W.M. Marr, *Rev. Sci. Instrum.* **71**, 2196 (2000)
- S. Shoji, *Electron. Commun. Jpn.* **2**, **82**, 21 (1999)
- F. Vajda, *Mathematical Modelling and Simulation of Industrial and Economic Processes*, IEE Colloquium on 1/1 (1994).
- M.M. Wang, E. Tu, D.E. Raymond, J.M. Yang, H.C. Zhang, N. Hagen, B. Dees, E.M. Mercer, A.H. Forster, I. Kariv, P.J. Marchand, W.F. Butler, *Nat. Biotechnol.* **23**, 83 (2005)
- J. Wietzorrek, M. Stadler, V. Kachel, *Oceans Engineering for Today's Technology and Tomorrow's Preservation* **1**, 1/688 (1994).
- H.-S. Wu, J. Barba, J. Gil, *IEEE Trans. Biomed. Eng.* **45**, 400 (1998)
- C.Q. Yi, C.W. Li, S.L. Ji, M.S. Yang, *Anal. Chim. Acta* **560**, 1 (2006)